Magneto-elastic coupling in compressed Fe_7C_3 supports carbon in Earth's inner core

Bin Chen,[1] Lili Gao,[2] Barbara Lavina,[3] Przemyslaw Dera,[4] Esen E. Alp,[2] Jiyong Zhao,[2] and Jie Li[1]

[1] The nature of light element(s) in the core holds key to our understanding of Earth's history of accretion and differentiation, but the core composition remains poorly constrained. Carbon has been proposed to be a major constituent of the inner core, with broad implications for the global carbon cycle, the budget of volatiles in the Earth and origin of carbon-based life in the Solar System. However, existing estimates of the inner core's carbon content remain highly controversial because of poor constraints on the behavior of compressed iron carbides. Here we investigated the structure, elasticity, and magnetism of Eckstrom-Adcock carbide Fe_7C_3 up to core pressures, using synchrotron-based single-crystal X-ray diffraction and Mössbauer spectroscopy techniques. We detected two discontinuities in the compression curve up to 167 gigapascals (GPa), the first of which corresponds to a magnetic collapse between 5.5 and 7.5 GPa and is attributed to a ferromagnetic to paramagnetic transition. At the second discontinuity near 53 GPa, Fe_7C_3 softens and exhibits Invar behavior, presumably caused by a high-spin to low-spin transition. Considering the magneto-elastic coupling effects, an Fe_7C_3-dominant composition can match the density of the inner core, making the core potentially the largest reservoir of carbon in Earth. **Citation:** Chen, B., L. Gao, B. Lavina, P. Dera, E. E. Alp, J. Zhao, and J. Li (2012), Magneto-elastic coupling in compressed Fe_7C_3 supports carbon in Earth's inner core, *Geophys. Res. Lett.*, *39*, L18301, doi:10.1029/2012GL052875.

1. Introduction

[2] Carbon is considered a candidate light element in the Earth's iron-rich core mainly because it partitions strongly into molten iron (Fe) during core-mantle differentiation and helps explain the density deficit of the core [*Wood*, 1993; *Lord et al.*, 2009; *Nakajima et al.*, 2009]. On the basis of thermodynamic calculations, *Wood* [1993] predicted that under relevant conditions Fe_3C would be the first phase to crystallize from the Earth's molten core to form the solid inner core. Recent studies found that at pressures above 7 GPa, Eckstrom-Adcock carbide Fe_7C_3 replaced Fe_3C to become the liquidus phase of the Fe-C binary system and hence the new candidate for the inner core [*Lord et al.*, 2009; *Nakajima et al.*, 2009]. Evaluating the scenario of Fe_7C_3-dominant inner core has broad implications for understanding the global carbon cycle, the budget of volatiles in the Earth, and how the planet accreted and differentiated [*Dasgupta et al.*, 2004]. Moreover, knowledge of the Earth's carbon content would provide unique ground-truth data to test models describing the origin of carbon in various stellar systems, its pathways from stars to Earth-like planets, and the role of carbon in the origin of life on exoplanets [*Swain et al.*, 2010].

[3] The hypothesized model of an Fe_7C_3-dominant inner core has been tested by comparing the density of Fe_7C_3 with that of the inner core, but existing studies reached inconsistent conclusions: An experimental investigation up to 71.5 GPa showed that Fe_7C_3 provides a good explanation for the density of the inner core [*Nakajima et al.*, 2011] whereas an *ab initio* calculation estimated that the volume fraction of Fe_7C_3 in the inner core is at most 18% [*Mookherjee et al.*, 2011]. The discrepancy arose from uncertainties in the nature and consequences of pressure-induced magnetic transitions. The experimental data revealed a pressure-induced ferromagnetic to paramagnetic transition at 18 GPa and 300 K, as indicated by anomalies in isothermal compression and thermal expansion behavior [*Nakajima et al.*, 2011]. On the contrary, the theoretical investigation found that Fe_7C_3 undergoes a high-spin to low-spin transition near 67 GPa and 0 K, with associated elastic softening [*Mookherjee et al.*, 2011]. Resolving the effects of magneto-elastic coupling is crucial for estimating the density of Fe_7C_3 under core conditions.

[4] To investigate the structure and elasticity of compressed Fe_7C_3, we carried out X-ray diffraction (XRD) measurements on single crystals of Fe_7C_3 immersed in a neon pressure-transmitting medium using synchrotron radiation and diamond-anvil cell techniques (Figure 1a and Figure S1 in Text S1). A parallel study was conducted to examine its magnetic properties using the synchrotron Mössbauer spectroscopy (SMS) method.

2. Experimental Methods

[5] An Fe_7C_3 sample was synthesized in a multi-anvil apparatus from an iron (Fe) wire placed in a graphite capsule at 7 GPa and 1623 K for 7 hours. A few grains of approximately $20 \times 20 \times 10$ μm in size were handpicked and verified as single crystals of Fe_7C_3 through synchrotron XRD analyses. High pressure was generated using symmetric diamond anvil cells (DAC). *In situ* single-crystal XRD

[1]Department of Earth and Environmental Sciences, University of Michigan, Ann Arbor, Michigan, USA.
[2]Advanced Photon Source, Argonne National Laboratory, Argonne, Illinois, USA.
[3]Department of Physics and Astronomy, University of Nevada, Las Vegas, Nevada, USA.
[4]Center for Advanced Radiation Sources, University of Chicago, Argonne National Laboratory, Argonne, Illinois, USA.

Corresponding author: B. Chen, Department of Earth and Environmental Sciences, University of Michigan, 1100 N. University Ave., Ann Arbor, MI 48109, USA. (binchen@umich.edu)
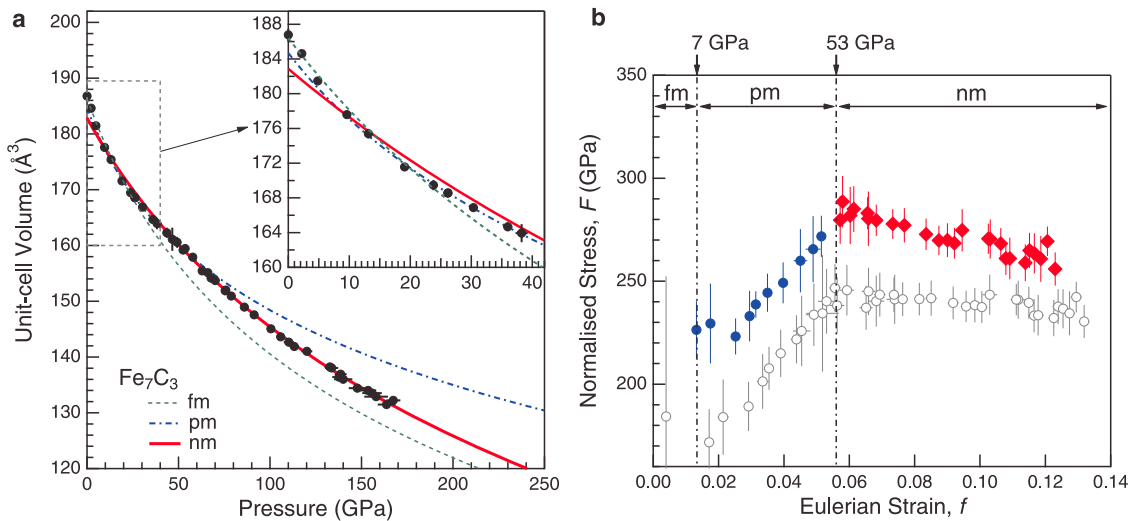
Figure 1. Compression behavior of Fe_7C_3 at 300 K. (a) Unit-cell volume of Fe_7C_3 up to 167 GPa at 300 K determined from the X-ray diffraction measurements (filled circles). The dashed green curve represents the 3rd–order Birch-Murnaghan equation of state (BM-EOS) of fm-Fe_7C_3 (1 bar to 7 GPa) according to *Nakajima et al.* [2011], as it cannot be constrained by the data collected in this study. The dash-dotted blue and solid red curves represent the BM-EOS fits to the data for pm-Fe_7C_3 (7–53 GPa) and nm-Fe_7C_3 (53–167 GPa), respectively. Here fm, pm and nm refer to ferromagnetic, paramagnetic, and non-magnetic, respectively. See text and Figure 2 for the assignment of magnetic phases. (b) Finite Eulerian strain (F) as a function of normalized stress (f). The dash-dotted lines mark the boundaries between the fm-, pm-, and nm-phases, as indicated by abrupt changes in the slopes of the f-F plot calculated using the unit-cell volume of Fe_7C_3 at ambient condition (open gray circles). Solid blue circles and red diamonds represent the f-F plots of pm-Fe_7C_3 and nm-Fe_7C_3, respectively.

measurements were carried out at beamlines 13-BM-D, 13-ID-D and 16-BM-D of APS. The XRD patterns were recorded on an MAR345 image plate detector or a charge coupled device (CCD) detector while the sample was rotated over an omega range of ±13–$16°$. Typical exposure time is 30 s per degree in the step scan mode and 600–900 s in the wide scan mode. Parallel SMS measurements were carried out on the same samples at beamline 3-ID-B of APS, with the storage ring operating in a top-up mode with 24 bunches separated by 153 ns. The X-ray energy was 14.4125 keV, corresponding to a wavelength of $\lambda = 0.8603$ Å. The focused X-ray beam was less than 10 μm in diameter with an energy resolution of 1 meV. Data were collected with an avalanche photodiode detector (APD), which was placed along the beam in the forward direction. Typical data collection time varied from 0.5 to 3 hours. Detailed methods are available in the auxiliary material.[1]

3. Results and Discussion

[6] Our ambient condition single-crystal XRD data confirmed that Fe_7C_3 adopted a hexagonal structure with the space group $P6_3mc$ and unit-cell parameters $a = 6.888$ (±0.006) Å and $c = 4.545(\pm0.011)$ Å [*Herbstein and Snyman*, 1964]. The structure remains stable up to 167 GPa at 300 K (Figure S1 and Table S1 in Text S1), but two discontinuities in the compression curve were detected using the normalized pressure (F) versus Eulerian strain (f) plot [*Angel*, 2001], which shows changes in the slope from negative (corresponding to $K' < 4$, where K' is the pressure derivative of bulk modulus) to positive ($K' > 4$) near 7 GPa, and then

to negative again near 53 GPa (Figure 1b). As a result, three distinct equations of state (EOS) are required to fit the compression data over the entire pressure range (Figure 1a). The data below 7 GPa are not fitted because of sparse data coverage within the narrow pressure range of this phase (Figure 1a). The data between 7 and 53 GPa yield $K_0 = 201(\pm12)$ GPa, $K' = 8.0(\pm1.4)$, and $V_0 = 184.69(\pm0.16)$ Å³ from Birch-Murnaghan (BM) EOS fitting, and those above 53 GPa are fitted with $K_0 = 307(\pm6)$ GPa, $K' = 3.2(\pm0.1)$, and $V_0 = 182.87(\pm0.38)$ Å³ (Table S2 in Text S1).

[7] A comparison of the compression curve with the SMS spectra reveals that the low-pressure discontinuity coincides with a magnetic collapse, which manifests as the disappearance of fast oscillations at pressures between 5.5 and 7.5 GPa in the SMS spectra (Figure 2). A magnetic collapse may result from a loss of magnetic ordering, or from a high-spin to low-spin transition of Fe. Previous studies associated elastic stiffening in Fe_7C_3 with ferromagnetic to paramagnetic transition, whereas elastic softening is linked to spin transition [*Mookherjee et al.*, 2011; *Nakajima et al.*, 2011]. For this reason, we attribute the observed magnetic collapse to a transition from ferromagnetic to paramagnetic phase, resulting from a negative pressure dependence of the Curie temperature [*Nakajima et al.*, 2011]. The transition pressure, determined from experiments using a fluid neon pressure-transmitting medium and the SMS method, is significantly lower than 18 GPa according to the previous study using a solid MgO medium and the XRD method [*Nakajima et al.*, 2011]. Similar discrepancies exist among the reported pressures of magnetic collapse in Fe_3C, ranging from 5–6 GPa to 25 GPa [*Gao et al.*, 2008]. Regardless of the exact nature of the magnetic collapse, our data demonstrate that the post-collapse Fe_7C_3 is significantly stiffer and lighter than the
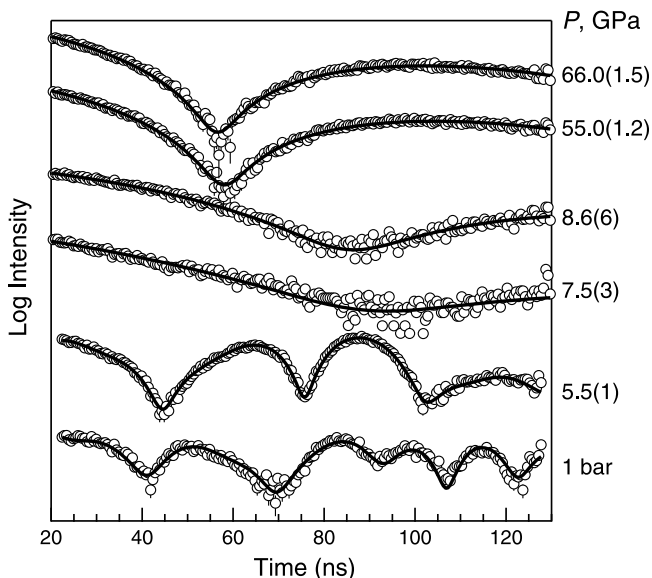
Figure 2. Synchrotron Mössbauer spectra of Fe$_7$C$_3$ (open circles) and fitting results with the best-fit parameters given in Table S3 in Text S1 (solid curves). Note that the disappearance of fast oscillations between 5.5 and 7.5 GPa indicates a loss of magnetism, and the differences between the spectra at 7.5 and 55.0 GPa reflect changes in the sample thickness and quadrupole splitting values.

lower-pressure phase when extrapolated to inner core pressures (Figure 1a).

[8] The high-pressure discontinuity in the compression curve near 53 GPa is interpreted as a result of high-spin to low-spin transition of Fe in Fe$_7$C$_3$, which was predicted to occur at 67 GPa and 0 K according to the theoretical study [*Mookherjee et al.*, 2011]. Across the discontinuity the quadrupole splitting values increase considerably (Figure S2 and Table S2 in Text S1). Moreover, the pressure dependence of the axial ratio a/c becomes smaller, similar to that calculated for the spin transition from ferromagnetic to nonmagnetic phase (Figure 3a). The transition leads to elastic softening in Fe$_7$C$_3$ as indicated by a drop in K (Figure 3b), which is consistent with the recent reports on pressure-induced Invar behavior resulting from high-spin to low-spin transition of Fe in metal alloys [*Dubrovinsky et al.*, 2001; *Winterrose et al.*, 2009].

[9] The unusual behavior of elastic stiffening followed by softening in compressed Fe$_7$C$_3$, presumably caused by tandem magnetic transitions under pressure, has not been observed in other Fe-rich alloys such as Fe$_3$C [*Gao et al.*, 2008], Fe$_3$S [*Lin et al.*, 2004], and FeH$_x$ [*Mao et al.*, 2004]. The discovery of the second transition in highly compressed Fe$_7$C$_3$, which was enabled by the synchrotron-based single-crystal XRD techniques, revealed that only the low-spin non-magnetic phase is relevant for testing the scenario of carbon-rich inner core. Using the derived EOS parameters of the nm-Fe$_7$C$_3$ and existing data on Fe [*Mao et al.*, 1990], we calculated the densities of Fe and Fe$_7$C$_3$ under core pressures and at 300 K. The effects of temperature were assessed using the Mie-Grüneisen-Debye (MGD) EOS, with the parameters of hcp-Fe from *Seagle et al.* [2006] and those of nm-Fe$_7$C$_3$ approximated by pm-Fe$_7$C$_3$ from *Nakajima et al.* [2011]. The estimated temperature at inner core boundary (ICB) ranges from about

5000 to 7000 K [*Boehler*, 1996]. At 5000 K, a mixture of 81–95% (by volume) Fe$_7$C$_3$ with hcp-Fe has the same density as the inner core [*Dziewonski and Anderson*, 1981]. The fraction of Fe$_7$C$_3$ to match the core density is 71–84% at 6000 K, and 62–74% at 7000 K. The close match in density between Fe$_7$C$_3$ and the inner core hinges upon the small K' of the nm-phase. In comparison, extrapolating the EOS of the pm-Fe$_7$C$_3$ to inner core condition would predict a density that is >11% below the PREM value, corresponding to a negligible amount of carbon in the inner core (Figure 4).

4. Conclusions

[10] On the basis of the EOS parameters of nm-Fe$_7$C$_3$ determined at pressures between 53 and 167 GPa and existing thermoelastic parameters [*Mao et al.*, 1990; *Seagle et al.*, 2006; *Nakajima et al.*, 2011], we estimated that the volume fraction of Fe$_7$C$_3$ in the inner core ranges from 62 to 95%, corresponding to a carbon content of 5.1–7.9% by weight. An Fe$_7$C$_3$-dominant inner core would be by far the largest reservoir of carbon in Earth, accounting for more than 90% of the planet's total carbon budget [*Dasgupta and Hirschmann*, 2010]. Our estimate represents an upper bound because we assumed that carbon was the sole light element in the core. More stringent assessment of the scenario of carbon-rich inner core awaits further studies. The nature of the discontinuities in the compression curve of Fe$_7$C$_3$ requires clarification using complementary techniques such as X-ray emission spectroscopy, which probes the local magnetic moment of Fe.
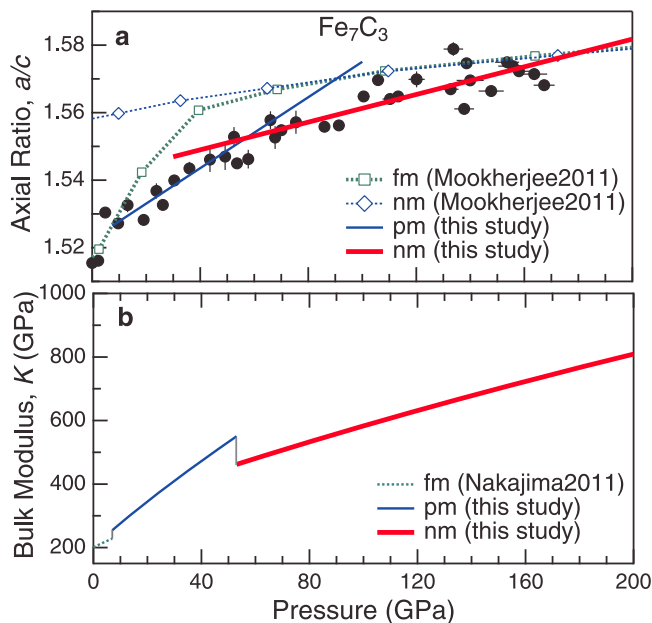

Figure 3. (a) Axial ratio a/c of Fe$_7$C$_3$ at 300 K as a function of pressure (filled circles), with least squares linear fits to the data of the pm-phase (thin blue line) and nm-phase (thick red line). Open squares and diamonds are theoretical results for the fm- and pm-phases, respectively [*Mookherjee et al.*, 2011]. (b) Isothermal bulk modulus (K) of Fe$_7$C$_3$ at 300 K as a function of pressure, calculated from the fitted BM-EOS parameters of the pm-phase (thin blue curve, this study), nm-phase (thick red curve, this study), and fm-phase (dotted curve, *Nakajima et al.* [2011]).
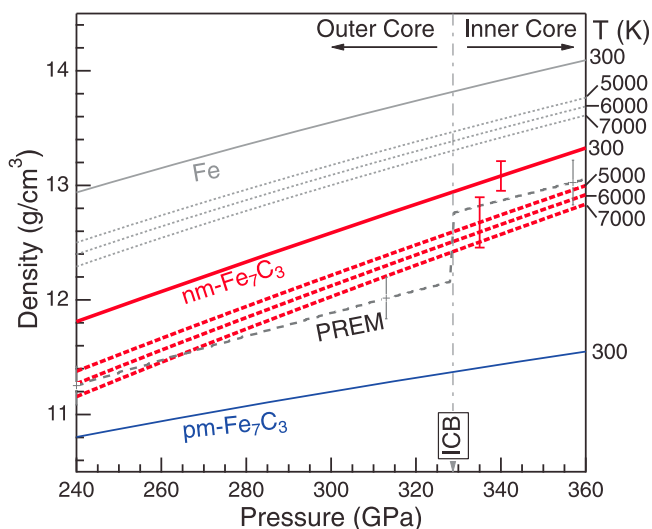
Figure 4. Calculated densities of Fe₇C₃ and hcp-Fe at 300 K (solid lines with red error bar) and high temperatures (dotted lines with red error bar) in comparison with the PREM model (dashed line with error bars representing ±1.5% uncertainties, *Dziewonski and Anderson* [1981]): Hcp-Fe (gray lines, *Mao et al.* [1990] and *Seagle et al.* [2006]); nm-Fe₇C₃ (thick red lines, this study), and pm-Fe₇C₃ (blue line, this study). The dash-dotted line indicates the pressure at the inner core boundary (ICB).

Additional measurements are also necessary to determine the influence of the magnetic transitions on the sound velocities and the effects of temperature on the magnetic transitions and thermoelastic parameters. A key criterion for the scenario of Fe₇C₃-dominant inner core, that it must be the major liquidus phase to crystallize from a liquid core containing Fe and one more lighter elements or impurities, will have to be further examined in order to constrain the core composition and understand the inventories and pathways of the Earth's deep carbon. This scenario should also satisfy with core convection and geodynamo models. Crystallization of Fe₇C₃ would concentrate carbon in the inner core while depleting the outer core in carbon, which disfavors the compositional convection by chemical buoyancy in the outer core. Existence of other light elements such as sulfur, however, could provide necessary chemical buoyancy for the core convection [e.g. *Wood*, 1993].

References

Angel, R. J. (2001), Equation of state, in *High-Pressure, High-Temperature Crystal Chemistry*, *Rev. Mineral. Geochem.*, vol. 41, edited by R. M. Hazen and R. T. Downs, pp. 41, 35–60, CRC Press, Boca Raton, Fla.

Boehler, R. (1996), Melting temperature of the Earth's mantle and core: Earth's thermal structure, *Annu. Rev. Earth Planet. Sci.*, 24, 15–40, doi:10.1146/annurev.earth.24.1.15.

Dasgupta, R., and M. M. Hirschmann (2010), The deep carbon cycle and melting in Earth's interior, *Earth Planet. Sci. Lett.*, 298(1–2), 1–13, doi:10.1016/j.epsl.2010.06.039.

Dasgupta, R., M. M. Hirschmann, and A. C. Withers (2004), Deep global cycling of carbon constrained by the solidus of anhydrous, carbonated eclogite under upper mantle conditions, *Earth Planet. Sci. Lett.*, 227(1–2), 73–85, doi:10.1016/j.epsl.2004.08.004.

Dubrovinsky, L. S., N. Dubrovinskaia, I. A. Abrikosov, M. Vennström, F. Westman, S. Carlson, M. van Schilfgaarde, and B. Johansson (2001), Pressure-induced invar effect in Fe-Ni alloys, *Phys. Rev. Lett.*, 86(21), 4851–4854, doi:10.1103/PhysRevLett.86.4851.

Dziewonski, A. M., and D. L. Anderson (1981), Preliminary reference Earth model, *Phys. Earth Planet. Inter.*, 25, 297–356, doi:10.1016/0031-9201(81)90046-7.

Gao, L., et al. (2008), Pressure-induced magnetic transition and sound velocities of Fe₃C: Implications for carbon in the Earth's inner core, *Geophys. Res. Lett.*, 35, L17306, doi:10.1029/2008GL034817.

Herbstein, F., and J. Snyman (1964), Identification of Eckstrom-Adcock iron carbide as Fe₇C₃, *Inorg. Chem.*, 3(6), 894–896, doi:10.1021/ic50016a026.

Lin, J.-F., Y. Fei, W. Sturhahn, J. Zhao, H. Mao, and R. J. Hemley (2004), Magnetic transition and sound velocities of Fe₃S at high pressure: Implications for Earth and planetary cores, *Earth Planet. Sci. Lett.*, 226(1–2), 33–40, doi:10.1016/j.epsl.2004.07.018.

Lord, O., M. Walter, R. Dasgupta, D. Walker, and S. M. Clark (2009), Melting in the Fe-C system to 70 GPa, *Earth Planet. Sci. Lett.*, 284, 157–167, doi:10.1016/j.epsl.2009.04.017.

Mao, H. K., Y. Wu, L. C. Chen, and J. F. Shu (1990), Static compression of iron to 300 GPa and Fe₀.₈Ni₀.₂ alloy to 260 GPa: Implications for compositions of the core, *J. Geophys. Res.*, 95, 21,737–21,742, doi:10.1029/JB095iB13p21737.

Mao, W. L., W. Sturhahn, D. L. Heinz, H.-K. Mao, J. Shu, and R. J. Hemley (2004), Nuclear resonant X-ray scattering of iron hydride at high pressure, *Geophys. Res. Lett.*, 31, L15618, doi:10.1029/2004GL020541.

Mookherjee, M., Y. Nakajima, G. Steinle-Neumann, K. Glazyrin, X. Wu, L. S. Dubrovinsky, C. McCammon, and A. I. Chumakov (2011), High-pressure behavior of iron carbide (Fe₇C₃) at inner core conditions, *J. Geophys. Res.*, 116, B04201, doi:10.1029/2010JB007819.

Nakajima, Y., E. Takahashi, T. Suzuki, and K. Funakoshi (2009), "Carbon in the core" revisited, *Phys. Earth Planet. Inter.*, 174(1–4), 202–211, doi:10.1016/j.pepi.2008.05.014.

Nakajima, Y., E. Takahashi, N. Sata, Y. Nishihara, K. Hirose, K. Funakoshi, and Y. Ohishi (2011), Thermoelastic property and high-pressure stability of Fe₇C₃: Implication for iron-carbide in the Earth's core, *Am. Mineral.*, 96(7), 1158–1165, doi:10.2138/am.2011.3703.

Seagle, C. T., A. J. Campbell, D. L. Heinz, and G. Shen (2006), Thermal equation of state of Fe₃S and implications for sulfur in Earth's core, *J. Geophys. Res.*, 111, B06209, doi:10.1029/2005JB004091.

Swain, M. R., et al. (2010), A ground-based near-infrared emission spectrum of the exoplanet HD 189733b, *Nature*, 463(7281), 637–639, doi:10.1038/nature08775.

Winterrose, M. L., M. S. Lucas, A. F. Yue, I. Halevy, L. Mauger, J. A. Muñoz, J. Hu, M. Lerche, and B. Fultz (2009), Pressure-induced invar behavior in Pd₃Fe, *Phys. Rev. Lett.*, 102, 237202, doi:10.1103/PhysRevLett.102.237202.

Wood, B. J. (1993), Carbon in the core, *Earth Planet. Sci. Lett.*, 117, 593–607, doi:10.1016/0012-821X(93)90105-I.